Published in final edited form as:
Curr Opin Cell Biol. 2007 October ; 19(5): 521. doi:10.1016/j.ceb.2007.09.001.

Gap Junction Channel Structure in the Early 21st Century: Facts and Fantasies

Mark Yeager[*] and **Andrew L. Harris**[‡]

[*] Department of Cell Biology, The Scripps Research Institute, 10550 N. Torrey Pines Rd., La Jolla, CA 92037, USA and Division of Cardiovascular Diseases, Scripps Clinic, 10666 N. Torrey Pines Rd., La Jolla, CA 92037, USA; e-mail: yeager@scripps.edu

[‡] Department of Pharmacology and Physiology, New Jersey Medical School of UMDNJ, 185 S. Orange Avenue, Newark, NJ 07103, USA; e-mail: aharris@umdnj.edu

Abstract

Gap junction channels connect the cytoplasms of adjacent cells through the end-to-end docking of single-membrane structures called connexons, formed by a ring of six connexin monomers. Each monomer contains 4 transmembrane α-helices, for a total of 24 α-helices in a connexon. The fundamental structure of the connexon pore is probably similar in unpaired connexons and junctional channels, and for channels formed by different connexin isoforms. Nevertheless, variability in results from structurally-focused mutagenesis and electrophysiological studies raise uncertainty about the specific assignments of the transmembrane helices. Mapping of human mutations onto a suggested C^{α} model predicts that mutations that disrupt helix-helix packing impair channel function. An experimentally determined structure at atomic resolution will be essential to confirm and resolve these concepts.

Keywords

gap junction channel; connexon; intercellular communication; electron microscopy; mutagenesis; computational modeling

Introduction

Gap junctions are specialized regions of cell-to-cell contact in which hexameric oligomers, called connexons, dock end-to-end noncovalently across a narrow extracellular gap. Hundred of channels cluster in so-called plaques, and the individual channels allow exchange of nutrients, metabolites, ions and small molecules of up to ≈1000 Da [1]. Coupling by gap junctions is a fundamental mechanism for cell-to-cell communication in higher organisms. More than 20 connexin isoforms have been identified to date in deuterostomes, from sea urchins to humans [2,3].

Each connexon, or hemichannel, is an annular assembly of six individual connexins that forms a pore through the plasma membrane. The different connexin isoforms can interact structurally

Correspondence to: Mark Yeager.

in various ways. Connexons may be homomeric or heteromeric, and junctional channels may be formed by connexons having the same or different compositions. The expression of multiple connexins in the same cell type, the multiplicity of isoforms, as well as their different structural combinations, likely provides exquisite "functional tuning" of this unique family of membrane channels.

The primary tools for structure analysis of gap junction channels include electron microscopy and image analysis [4–9], X-ray diffraction [10–12], nuclear magnetic resonance (NMR) spectroscopy [13–15] and atomic force microscopy (AFM) [16–18]. Mutagenic, biochemical and electrophysiological approaches have also been used to elucidate the structure-function relationships of gap junction channels. This review focuses on recent studies that illuminate the structure of connexin channels, drawing on maps derived by electron cryo-crystallography and on structurally focused mutagenesis and electrophysiological studies. The reader is also referred to reviews by Yeager and Nicholson [19], Harris [20], Sosinsky and Nicholson [21] and Kovacs et al. [22].

The connexon contains a ring of 24 α-helices

Hydropathy and topological analyses of various connexins suggest that each contains four transmembrane domains, referred to as M1, M2, M3 and M4, proceeding from the N- to the C-terminus [23]. Connecting the transmembrane domains are two extracellular loops (E1, connecting M1 to M2, and E2, connecting M3 to M4) and one cytoplasmic M2-M3 loop. Both the N- and C-termini reside in the cytoplasm [23–25]. The transmembrane domains and the extracellular loops display the highest conservation in sequence [26,27]. The most variable domains, both in length and sequence, are the cytoplasmic C-terminal domain and the cytoplasmic loop connecting M2 to M3.

The general higher-order structure of gap junction channels was first revealed by electron cryomicroscopy and image analysis of two-dimensional crystals at 19 Å resolution [4]. Two-dimensional projection maps at 7 Å resolution revealed superimposed α-helices that could only arise if the connexons are rotationally staggered by 30° around the 6-fold symmetry axis [5] (Figure 1a). Thereafter, a 3D map at 7.5 Å in-plane resolution showed that each connexon contains 24 rod-like densities readily interpreted as transmembrane α-helices [7] (Figure 1). The primary sequence identity of each transmembrane helix could not be assigned at this resolution, so they were arbitrarily designated A, B, C and D (Figure 2). The map revealed that the pore of each connexon had a funnel-like shape, with the wide end on the cytoplasmic side of each bilayer. The wall of the pore at the cytoplasmic end was defined by 12 α-helices, two from each subunit (helices B and C in Figure 2). At the extracellular end, the pore was bounded primarily by helix C. This helix was tilted through most of the length of the pore with a distinct kink at the extracellular end where it became perpendicular to the plane of the membrane.

The resolution of the cryoEM map did not allow visualization of amino acid side chains, precluding definitive assignment of M1-M4 to specific transmembrane sequences. Nevertheless, physiological and biochemical experiments, in concert with mutagenesis, have been employed to identify pore-lining residues and segments. For connexin channels, these studies have their origins in two inferences. One inference, made by Milks et al. [23], was that M3 is a pore-lining helix because it contains a segment in which hydrophilic residues are found at every third or fourth position. If this region were α-helical, this would provide an energetically favorable wall for an aqueous pore. The second inference, made by Harris et al. [28] from electrophysiological studies, was that the voltage sensing regions of connexin channels were within the aqueous pore itself, rather than in a separate, voltage-sensing domain, as is the case for other voltage dependent channels [29,30]. This means that studies of the molecular basis of voltage sensitivity could inform studies of the pore, and *vice versa*.

The first experiments to provide data relevant to the latter assertion were those of Verselis, Bargiello and colleagues, beginning in 1994. Their work showed that single amino acid charge changes in the ostensibly cytoplasmic, amino-terminal (NT) domain of a Cx32 variant could actually reverse the polarity of voltage that caused the channels to close [31–34]. NMR spectroscopy of an NT peptide suggested that it could adopt a bent conformation allowing NT amino acids to access the cytoplasmic vestibule of the pore [35]. Studies of Cx40 [36] and Cx56 [37] also suggested that NT residues were involved in both voltage sensing and pore properties. Interestingly, mutations at the M1/E1 border in Cx32 also affected the polarity of voltage sensitivity [31] and in Cx56 altered voltage gating [37]. These data implicate the two extramembrane segments on either end of M1 as involved in the pore, and inspired a set of domain swaps, point mutations, and studies using the substituted cysteine accessibility method (SCAM) on this and other regions.

Regions in NT, M1, E1 and/or M3 have been implicated in lining the pore

Several domain swap studies showed that the single channel conductance of connexin pores is a property that can be transferred between channels by exchange of M1, particularly its second half (Cx46, Cx37, Cx32; [38,39]). Other domain swap studies showed that the charge selectivity of connexin pores can be controlled by E1 (Cx46, Cx32; [40]), suggesting that E1 contributes to the pore wall. Point mutations in the NT produced changes in the single channel current-voltage relations consistent with electrostatic effects on the permeating ions (Cx32; [32]). Mutations at two positions in the NT of Cx40 showed that they were essential for spermine block of these channels (the block thought to be at the cytoplasmic vestibule; [36]). Taken together, these data suggest that the NT, the second half of M1 and at least the initial part of E1 are directly involved in defining the conductance properties of connexin pores.

Involvement of the second half of M1 received experimental support from SCAM studies utilizing two types of thiol-reactive reagents, at both the macroscopic and single channel levels of analysis, carried out on single connexons. Studies using the large thiol reagent MBB (maleimidobutyryl biocytin) identified two sites of reaction in the second half of M1 (Cx46, Cx32; [41]). Similar studies of M3 were inconclusive due to smaller effects.

A set of MTS (methanethiosulfonate) reagents, which are much smaller than MBB, applied to single connexons in excised patches reacted very rapidly at a series of sites in the second half of M1, extending up to the M1/E1 border (Cx46; [42]). Modification by MTS reagents of different charge altered the single channel current-voltage relations in a manner that suggested direct electrostatic interaction with the current-carrying ions. No evidence of modification was found for sites in the second half of M3.

In contrast to these findings, measurements of macroscopic current with application of MBB to junctional channels in a cut-open paired oocyte preparation implicated M3 (Cx32; [43]), originally suggested by hydrophobicity analysis of connexin sequences. All four transmembrane domains were tested for accessibility to MBB. A series of reactive sites separated by two to three amino acids were identified in M3. Several sites in M1 were also reactive, but they were viewed as accessible in the closed but not the open state.

The different implications for pore lining segments would be easily resolved if one could attribute them to differences between the specific connexins studied and/or the fact that one set of data is from single connexons and the other from junctional channels. Unfortunately, these simple explanations do not seem to apply. There are two phylogenetic groups of connexins, with Cx26 and Cx32, members of one group and Cx43 a member of the other [44,45]. While there must be some structural differences to account for different limiting pore diameters and charge selectivities, it would be truly remarkable if the fundamental organization and packing of the transmembrane helices were different. More to the point, the transmembrane

densities derived from cryo-EM of the M34A mutant of Cx26 [9] are virtually identical to those derived from cryo-EM of Cx43 [7].

By the same token, there must be some differences in the pore-lining structures between unpaired connexons and connexons in junctional channels, simply by virtue of the docking interactions at the extracellular end of the connexons. Again, it would be remarkable if this resulted in wholesale differences in transmembrane packing. In fact, a host of data from measurements of unitary conductances, voltage sensitivities, pharmacological sensitivities and other functional properties of single connexons and junctional channels suggest that this does not occur [20,42]. Since the differences cannot be readily explained by the considerations above, they may arise from some combination of the differences in the thiol-reactive reagents used, the different physical configurations of the experiments, and the relative reliabilities, sources of artifact and constraints inherent in the two experimental protocols. Simply put, these different experiments may be revealing different kinds of information about the channels.

In most SCAM studies, the thiol-modifying reagent is presumed to have free access to the molecule of interest. Therefore the rate of modification is considered to be a function of the molecular accessibility of the reagent to the specific group modified. Accessibility can be a function of steric impediment (e.g., the residue is buried deep in the protein interior) and/or a function of the structural states occupied by the target molecule during exposure to the reagent (e.g., how much time a channel is in an open versus closed state). Thus, if a channel is open 90% of the time during incubation with an MTS reagent, one would expect the positions most “accessible” (i.e., most rapidly modified) to MTS modification to be those exposed to the pore lumen when the channel is open, as opposed to those uniquely exposed when closed.

These considerations raise two potential concerns about the SCAM data from the paired oocytes. One is the long time (20 minutes) of exposure to MBB. It is unclear how much of this time was required for diffusion of the large MBB reagent to the junctional molecules through residual oocyte cytoplasmic components. If the delay of action can be thus accounted for, it is not a concern. However, if it takes minutes for modification after reaching the junctions, there is concern that the reactive sites are not sufficiently accessible for the results to be specific for exposed (i.e., pore-lining) residues. The other concern is about the relatively small change in macroscopic currents as a result of modification. On a single channel level, one expects that modification of Cx32 with MBB within the pore will substantially decrease unitary conductance (it decreases Cx46 conductance 80%; Pfahnl and Dahl [46]). However, the effects on the currents in the oocyte system were much smaller (15–20%). This can mean that either the modification is occurring far enough outside the pore that the MBB only slightly occludes it, or that only a small fraction of the channels are being modified, as if a large fraction of the channels are inaccessible to the reagent. While each of these concerns may be satisfactorily explained, at present they remain unresolved, and stand in contrast to the rapid and dramatic effects seen with the MTS reagents at the single channel level of resolution.

A C^{α} model suggests that mutations that disrupt helix-helix packing interfere with channel function

Clearly, an essential challenge is to utilize the existing 3D cryoEM map and the existing mutagenesis, physiological and amino acid sequence data to come to a consensus about which parts of which domains line the pore. The key difficulties are that the map (1) is of necessity a snapshot of a single structural state, and (2) it may not correspond to the dominant state probed by the mutagenesis/physiological studies. For these reasons, it is perhaps unrealistic to expect the two sets of data to be entirely reconciled; the functional state of the 3D map is uncharacterized, and the SCAM studies have their own potential ambiguities of interpretation.

With these caveats in mind, an improved cryo-EM map (with in-plane resolution of 5.7 Å and vertical resolution of 19.8 Å) was used as a basis from which to generate a C^{α} model for the transmembrane domains within a connexon [8] (Figure 3). The two most important new features of this model were proposals for the orientation and sequence identity of the transmembrane helices. For membrane proteins, evolutionarily conserved amino acids are more likely to mediate protein packing interactions, and variable residues are more likely to face the lipid [47]. On the basis of the relative spatial locations of conserved and variable residues within the connexin family, as well as some of the SCAM data, the primary sequence of transmembrane segments M1–M4 was assigned to the observed α-helices in the map (*A*=*M*2, *B*=*M*1, *C*=*M*3, *D*=*M*4) (Figure 2). This assignment predicted that M4 was the helix on the perimeter of the connexon. Support for this inference has been provided by experiments in which M4 of Cx43 was replaced with polyalanine without interfering with gap junctional communication [48]. The relative rotation angles of the α-helices fitted into the density map were estimated by analysis of evolutionary conservation and hydrophobicity of amino acid residues. We note that although this is the most well-defined model for the transmembrane domains of gap junctions as of this writing, the conformations of the amino acid side chains remain undetermined. In addition, the α-helical rods in the cryo-EM density map display curvature not reflected in the idealized C^{α} model of Fleishman et al. [8]. With these provisos, the location of mutations causing human diseases such as nonsyndromic deafness and Charot-Marie-Tooth disease could be mapped onto the C^{α} model (Figure 3). There was a surprising concentration of mutations at helix-helix interfaces, suggesting that disruption of helix packing interferes with channel function.

We note that the helical assignment in Fleishman et al. [8] differs from that deduced from the oocyte SCAM experiments [43] in which M1 and M2 were reversed (i.e., *A*=*M*1, *B*=*M*2) (Figure 2), and from that suggested by the single channel SCAM and domain swap studies, which implicate M1 as pore-lining. As discussed above, these discrepancies might be attributed to methodological differences or to possible differences in conformation, such as the latter representing an open conformation and the former a closed conformation. Another possibility is the presence of conformational flexibility or “breathing” that would create transient solvent crevices between α-helices that would allow labeling of residues that do not line the pore.

While progress has been made regarding assignment of the α-helices, there remains ambiguity as to the exact molecular boundary of the individual monomers, since the connecting loops between helices could not be resolved. The packing of the 24 α-helices within the 6-fold symmetric connexon can accommodate several possible molecular boundaries. Scrutiny of the density map and exclusion of models that require crossovers of the E1 and E2 loops suggests that the most likely molecular boundaries are a closely-packed 4-helix bundle or a more loosely packed “checkmark” arrangement [7], shown in Figure 2 for the helical assignments of Fleishman et al. [8] (blue) and Skerrett et al. [43] (green). A map at high resolution will be required to resolve these possibilities.

The N-terminus may form a plug that blocks Cx26 channels

NMR spectroscopy of a 13 residue peptide corresponding to the N-terminal domain of Cx26 displayed a two-turn α-helix, which then unraveled into a flexible loop-like structure [35]. It was hypothesized that this short NT helix is oriented parallel to the transmembrane helices lining the entrance to the pore, thus forming part of the conduction path and contributing to the voltage dependence of the channel. Support for this model is suggested by recent cryoEM studies of the M34A mutant of Cx26 [9]. In contrast to previous cryoEM studies of two-dimensional crystals derived from native plasma membranes [5,7,8], these two-dimensional crystals were generated by reconstituting detergent-solubilized, purified, recombinant Cx26 into lipid bilayers. Surprisingly, the connexons appeared to redock during the reconstitution,

thereby forming dodecameric channels (Figure 4). A surprising and unexpected feature of the map was a plug of density in the cytoplasmic mouth of the pore. Several experimental conditions favored a closed conformation of Cx26 (e.g., use of the M34A mutant, low pH, aminosulfonate buffer, carbenoxolone and high Ca^{++} and Mg^{++}). The simplest interpretation is that the plug represents an aggregate of the amino-termini, suggesting a simple mechanism for pore gating. The carboxy-tail domain has been proposed to mediate low pH gating by interacting with the M2-M3 loop [49]. However, this mechanism has not been demonstrated for Cx26, and Cx26 does not contain the required C-terminal segment. Confirmation of the chemical identity of the plug requires a bona fide, high resolution map so that the amino acids in the NT could be identified. Alternatively, a difference 3D map between Cx26 with and without the NT, even at an intermediate resolution such as 7 Å, would confirm that the plug is formed by association of NT peptides.

Conclusions

The last decade has seen impressive progress in the analysis of several classes of membrane proteins, including reaction centers, porins, ligand-gated channels, voltage-gated channels, transporters and aquaporins [50]. By comparison, the tempo of discovery in the gap junction channel field has been slower. Possible reasons include difficulties with expression of engineered connexins with sufficient stability and quantity to allow detailed biochemical and biophysical analysis, difficulties in performing electrophysiological studies on a channel that spans two membranes, and lack of a repertoire of pharmacological agents to probe channel function. Nevertheless, recent electrophysiological, biochemical and biophysical studies, and analysis of engineered and pathological mutations, have yielded a working model for the general molecular design of gap junction channels, even if there is ambiguity in specific helix assignments. There is currently no information on amino-acid side-chain conformations, which will be essential to understand the molecular basis of (1) the stability and selectivity in docking of connexons, (2) mechanisms of gating, (3) mechanisms of molecular permselectivitiy, and (4) the ability to form homomeric and heteromeric, as well as homotypic and heterotypic channels. Structural data at atomic resolution are required to gain insight into these unique functional properties of gap junction channels.

Acknowledgments

This work was supported by NIH grants RO1HL48908 (M.Y.), RO1GM36044 (A.L.H.) and RO1NS056509 (A.L.H.). We thank Julio Kovacs, Kenton Baker and Michael E. Pique for preparation of Figures 1, 2, and 3, respectively. We thank Atsunori Oshima and Yoshinori Fujiyoshi for providing Figure 4.

Abbreviations

AFM	atomic force microscopy
cryoEM	electron cryomicroscopy
Cx	connexin
3D	three-dimensional
E1	E2, first and second extracellular loops, respectively, of a connexin subunit
M1	M2, M3, M4, first, second, third and fourth transmembrane domains, respectively, of a connexin subunit
MBB	maleimidobutyryl biocytin
MTS	methanethiosulfonate
NMR	nuclear magnetic resonance

NT	amino-terminal domain of a connexin
SCAM	substituted cysteine accessibility method

References

1. Loewenstein WR. Junctional intercellular communication: the cell-to-cell membrane channel. Physiol Rev 1981;61:829–913. [PubMed: 6270711]
2. Bruzzone R, White TW, Paul DL. Connections with connexins: the molecular basis of direct intercellular signaling. Eur J Biochem 1996;238:1–27. [PubMed: 8665925]
3. Gerido DA, White TW. Connexin disorders of the ear, skin, and lens. Biochim Biophys Acta 2004;1662:159–170. [PubMed: 15033586]
4. Unwin PN, Ennis PD. Two configurations of a channel-forming membrane protein. Nature 1984;307:609–613. [PubMed: 6320017]
5. Unger VM, Kumar NM, Gilula NB, Yeager M. Projection structure of a gap junction membrane channel at 7 A resolution. Nat Struct Biol 1997;4:39–43. [PubMed: 8989321]
6. Perkins GA, Goodenough DA, Sosinsky GE. Formation of the gap junction intercellular channel requires a 30° rotation for interdigitating two apposing connexons. J Mol Biol 1998;277:171–177. [PubMed: 9514740]
7. Unger VM, Kumar NM, Gilula NB, Yeager M. Three-dimensional structure of a recombinant gap junction membrane channel. Science 1999;283:1176–1180. [PubMed: 10024245]
8. Fleishman SJ, Unger VM, Yeager M, Ben-Tal N. A C^{α} model for the transmembrane alpha helices of gap junction intercellular channels. Mol Cell 2004;15:879–888. [PubMed: 15383278]

9••. Oshima A, Tani K, Hiroaki Y, Fujiyoshi Y, Sosinsky GE. Three-dimensional structure of a human connexin26 gap junction channel reveals a plug in the vestibule. Proc Natl Acad Sci U S A 2007;104:10034–10039. CryoEM and image analysis of 2D crystals formed by reconstitution of recombinant Cx26 into lipid bilayers revealed a plug of density in the center of the pore, thought to arise from an aggregate of N-terminal domains. Notably, this plug was not seen in cryoEM maps of Cx43[5,7,8]. [PubMed: 17551008]

10. Unwin PN, Ennis PD. Calcium-mediated changes in gap junction structure: Evidence from the low angle X-ray pattern. J Cell Biol 1983;97:1459–1466. [PubMed: 6630291]
11. Tibbitts TT, Caspar DLD, Phillips WC, Goodenough DA. Diffraction diagnosis of protein folding in gap junction connexons. Biophys J 1990;57:1025–1036. [PubMed: 2160297]
12. Makowski L, Caspar DLD, Phillips WC, Goodenough DA. Gap junction structures. II. Analysis of the X-ray diffraction data. J Cell Biol 1977;74:629–645. [PubMed: 889612]

13•. Sorgen PL, Duffy HS, Sahoo P, Coombs W, Delmar M, Spray DC. Structural changes in the carboxyl terminus of the gap junction protein connexin43 indicates signaling between binding domains for c-Src and zonula occludens-1. J Biol Chem 2004;279:54695–54701. NMR spectroscopy of the isolated C-terminus of Cx43 showed that the polypeptide is mostly disordered, with the exception of two short non-association helical stretches (amino acids 315–326 and 340–348), whose structure depends on pH. These authors proposed that these helical regions may dimerize and be important in gating. [PubMed: 15492000]

14. Sorgen PL, Duffy HS, Spray DC, Delmar M. pH-dependent dimerization of the carboxyl terminal domain of Cx43. Biophys J 2004;87:574–581. [PubMed: 15240490]
15. Duffy HS, Sorgen PL, Girvin ME, O'Donnell P, Coombs W, Taffet SM, Delmar M, Spray DC. pH-dependent intramolecular binding and structure involving Cx43 cytoplasmic domains. J Biol Chem 2002;277:36706–36714. [PubMed: 12151412]
16. Müller DJ, Hand GM, Engel A, Sosinsky GE. Conformational changes in surface structures of isolated connexin 26 gap junctions. EMBO J 2002;21:3598–3607. [PubMed: 12110573]

17•. Yu J, Bippes CA, Hand GM, Muller DJ, Sosinsky GE. Aminosulfonate modulated pH-induced conformational changes in connexin26 hemichannels. J Biol Chem 2007;282:8895–8904. In a previous study [16], this group used AFM to visualize Ca^{++}-induced conformational changes in the extracellular surface of Cx26. In this study, pH-induced closure of Cx26 channels was observed in

aminosulfonate buffers such as HEPES, but not in non-aminosulfonate buffers. [PubMed: 17227765]

18•. Liu F, Arce FT, Ramachandran S, Lal R. Nanomechanics of hemichannel conformations: Connexin flexibility underlying channel opening and closing . J Biol Chem 2006;281:23207–23217. AFM was used to show that the carboxy-tail of Cx43 is more distensible than the E1 extracellular loop. By the use of carboxy-tail antibodies, the stretch length and energy required for stretching the carboxy-tail supported a particle-receptor model for gating [45]. [PubMed: 16769719]

19. Yeager, M.; Nicholson, BJ. Structure and biochemistry of gap junctions. In: Hertzberg, E., editor. Gap Junctions. Vol. 30 of Advances in Molecular and Cell Biology. JAI Press; 2000. p. 31-98.

20. Harris AL. Emerging issues of connexin channels: biophysics fills the gap. Q Rev Biophys 2001;34:325–472. [PubMed: 11838236]

21. Sosinsky GE, Nicholson BJ. Structural organization of gap junction channels. Biochim Biophys Acta 2005;1711:99–125. [PubMed: 15925321]

22. Kovacs JA, Baker KA, Altenberg GA, Abagyan R, Yeager M. Molecular modeling and mutagenesis of gap junction channels. Prog Biophys Mol Biol 2007;94:15–28. [PubMed: 17524457]

23. Milks LC, Kumar NM, Houghten R, Unwin N, Gilula NB. Topology of the 32-kd liver gap junction protein determined by site-directed antibody localizations. EMBO J 1988;7:2967–2975. [PubMed: 2460334]

24. Yancey SB, John SA, Lal R, Austin BJ, Revel J-P. The 43-kD polypeptide of heart gap junctions: immunolocalization, topology, and functional domains. J Cell Biol 1989;108:2241–2254. [PubMed: 2472402]

25. Yeager M, Gilula NB. Membrane topology and quaternary structure of cardiac gap junction ion channels. J Mol Biol 1992;223:929–948. [PubMed: 1371548]

26. Beyer EC, Paul DL, Goodenough DA. Connexin43: A protein from rat heart homologous to a gap junction protein from liver. J Cell Biol 1987;105:2621–2629. [PubMed: 2826492]

27. Kumar NM, Gilula NB. Cloning and characterization of human and rat liver cDNAs coding for a gap junction protein. J Cell Biol 1986;103:767–776. [PubMed: 2875078]

28. Harris AL, Spray DC, Bennett MV. Kinetic properties of a voltage-dependent junctional conductance. J Gen Physiol 1981;77:95–117. [PubMed: 6259275]

29. Long SB, Campbell EB, Mackinnon R. Crystal structure of a mammalian voltage-dependent *Shaker* family K+ channel. Science 2005;309:897–903. [PubMed: 16002581]

30. Tombola F, Pathak MM, Isacoff EY. How does voltage open an ion channel? Annu Rev Cell Dev Biol 2006;22:23–52. [PubMed: 16704338]

31. Verselis VK, Ginter CS, Bargiello TA. Opposite voltage gating polarities of two closely related connexins. Nature 1994;368:348–351. [PubMed: 8127371]

32. Oh S, Rivkin S, Tang Q, Verselis VK, Bargiello TA. Determinants of gating polarity of a connexin 32 hemichannel. Biophys J 2004;87:912–928. [PubMed: 15298899]

33. Purnick PEM, Oh S, Abrams CK, Verselis VK, Bargiello TA. Reversal of the gating polarity of gap junctions by negative charge substitutions in the N-terminus of connexin 32. Biophys J 2000;79:2403–2415. [PubMed: 11053119]

34. Oh S, Abrams CK, Verselis VK, Bargiello TA. Stoichiometry of transjunctional voltage-gating polarity reversal by a negative charge substitution in the amino terminus of a connexin32 chimera. J Gen Physiol 2000;116:13–31. [PubMed: 10871637]

35. Purnick PE, Benjamin DC, Verselis VK, Bargiello TA, Dowd TL. Structure of the amino terminus of a gap junction protein. Arch Biochem Biophys 2000;381:181–190. [PubMed: 11032405]

36. Musa H, Fenn E, Crye M, Gemel J, Beyer EC, Veenstra RD. Amino terminal glutamate residues confer spermine sensitivity and affect voltage gating and channel conductance of rat connexin40 gap junctions. J Physiol 2004;557:863–878. [PubMed: 15107469]

37. Tong J-J, Ebihara L. Structural determinants for the differences in voltage gating of chicken Cx56 and Cx45.6 gap-junctional hemichannels. Biophys J 2006;91:2142–2154. [PubMed: 16798801]

38. Hu X, Dahl G. Exchange of conductance and gating properties between gap junction hemichannels. FEBS Lett 1999;451:113–17. [PubMed: 10371149]

39. Hu X, Ma M, Dahl G. Conductance of connexin hemichannels segregates with the first transmembrane segment. Biophys J 2006;90:140–150. [PubMed: 16214855]
40. Trexler EB, Bukauskas FF, Kronengold J, Bargiello TA, Verselis VK. The first extracellular loop domain is a major determinant of charge selectivity in connexin46 channels. Biophys J 2000;79:3036–3051. [PubMed: 11106610]
41. Zhou X-W, Pfahnl A, Werner R, Hudder A, Llanes A, Luebke A, Dahl G. Identification of a pore lining segment in gap junction hemichannels. Biophys J 1997;72:1946–1953. [PubMed: 9129799]
42••. Kronengold J, Trexler EB, Bukauskas FF, Bargiello TA, Verselis VK. Single-channel SCAM identifies pore-lining residues in the first extracellular loop and first transmembrane domains of Cx46 hemichannels. J Gen Physiol 2003;122:389–405. Application of charged MTS reagents to excised patches containing connexons showed rapid modification of sites in the second half of M1 and the initial portion of E1. Modification was assessed by changes in single channel current-voltage relations and conductance expected for electrostatic interaction of the charged MTS reagents with the current-carrying ions. No reactivity was seen in the corresponding segment of M3. [PubMed: 12975451]
43••. Skerrett IM, Aronowitz J, Shin JH, Cymes G, Kasperek E, Cao FL, Nicholson BJ. Identification of amino acid residues lining the pore of a gap junction channel. J Cell Biol 2002;159:349–360. SCAM analysis of all four transmembrane segments of junctional channels in a cut-open oocyte preparation showed periodic MBB reactivity over a substantial portion of M3. There was reactivity at a few sites in M1 and M2, not attributed to accessibility in the open state. [PubMed: 12403817]
44. Bennett MV, Zheng X, Sogin ML. The connexins and their family tree. Soc Gen Physiol Ser 1994;49:223–233. [PubMed: 7939897]
45. Kumar NM, Gilula NB. Molecular biology and genetics of gap junction channels. Semin Cell Biol 1992;3:3–16. [PubMed: 1320430]
46. Pfahnl A, Dahl G. Localization of a voltage gate in connexin46 gap junction hemichannels. Biophys J 1998;75:2323–2331. [PubMed: 9788927]
47. Baldwin JM. The probable arrangement of the helices in G protein-coupled receptors. EMBO J 1993;12:1693–1703. [PubMed: 8385611]
48. Bao X, Chen Y, Lee SH, Lee SC, Reuss L, Altenberg GA. Membrane transport proteins with complete replacement of transmembrane helices with polyalanine sequences remain functional. J Biol Chem 2005;280:8647–8650. [PubMed: 15596437]
49. Ek-Vitorín JF, Calero G, Morley GE, Coombs W, Taffet SM, Delmar M. pH regulation of connexin43: Molecular analysis of the gating particle. Biophys J 1996;71:1273–1284. [PubMed: 8874002]
50. Raman P, Cherezov V, Caffrey M. The Membrane Protein Data Bank. Cell Mol Life Sci 2006;63:36–51. [PubMed: 16314922]
51. Foote CI, Zhou L, Zhu X, Nicholson BJ. The pattern of disulfide linkages in the extracellular loop regions of connexin 32 suggests a model for the docking interface of gap junctions. J Cell Biol 1998;140:1187–1197. [PubMed: 9490731]

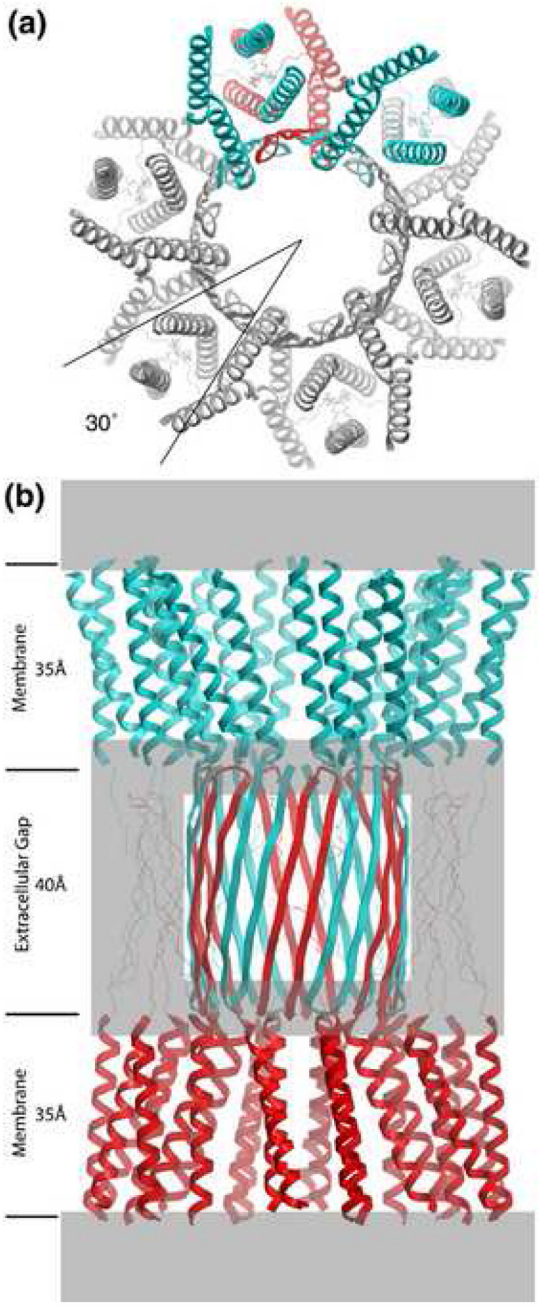

Figure 1.

Molecular design of gap junction channels. (a) Top view showing the 30 ° rotational stagger between docked connexons. Two subunits of the top connexon (in blue) are above one subunit of the bottom connexon (in red). The other subunits have been colored gray for clarity. The molecular boundary is depicted as a 4-helix bundle, but there are other possibilities (Figure 2). (b) Side view. The top connexon is in blue and the bottom one in red. Grayed areas denote parts of the structure that are most uncertain, especially the folding within the density at the boundary between the transmembrane assembly and the extracellular space. Putative β sheets corresponding to E1 (on the perimeter of the extracellular gap) are drawn with thin lines to emphasize this ambiguity. The E2 loops are depicted as an interdigitating β barrel [51]. Refer

to Figures 2 and 3 in reference [7] for the corresponding views of the 3D density map derived by electron cryo-crystallography. The dimensions for the transmembrane helical domain and the extracellular gap are approximate. From [22], reproduced by permission.

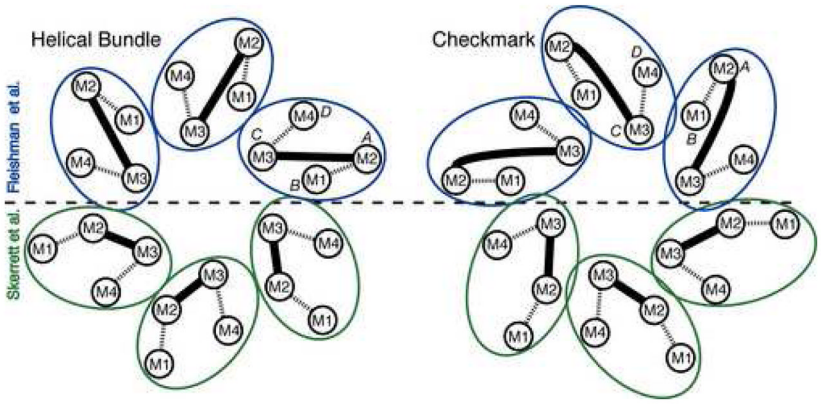

Figure 2.

Possible molecular boundaries for the connexin subunit include a helical bundle (left) and a "checkmark" (right) (following the naming of Unger et al. [7]). Each shows two assignments for the 4 transmembrane α-helices within each subunit, according to Fleishman et al. [8] (top, blue) and Skerrett et al. [43] (bottom, green). Dashed lines denote the extracellular loops, E1 and E2, and the solid lines denote the M2-M3 cytoplasmic loops. The α-helical rods designated A, B, C and D in the 3D density map derived by electron cryo-crystallography (Unger et al. [7] are also indicated. Both assignments shown designate M3 as the major pore lining helix, but other studies suggest M1, as discussed in the text. From [22], reproduced by permission.

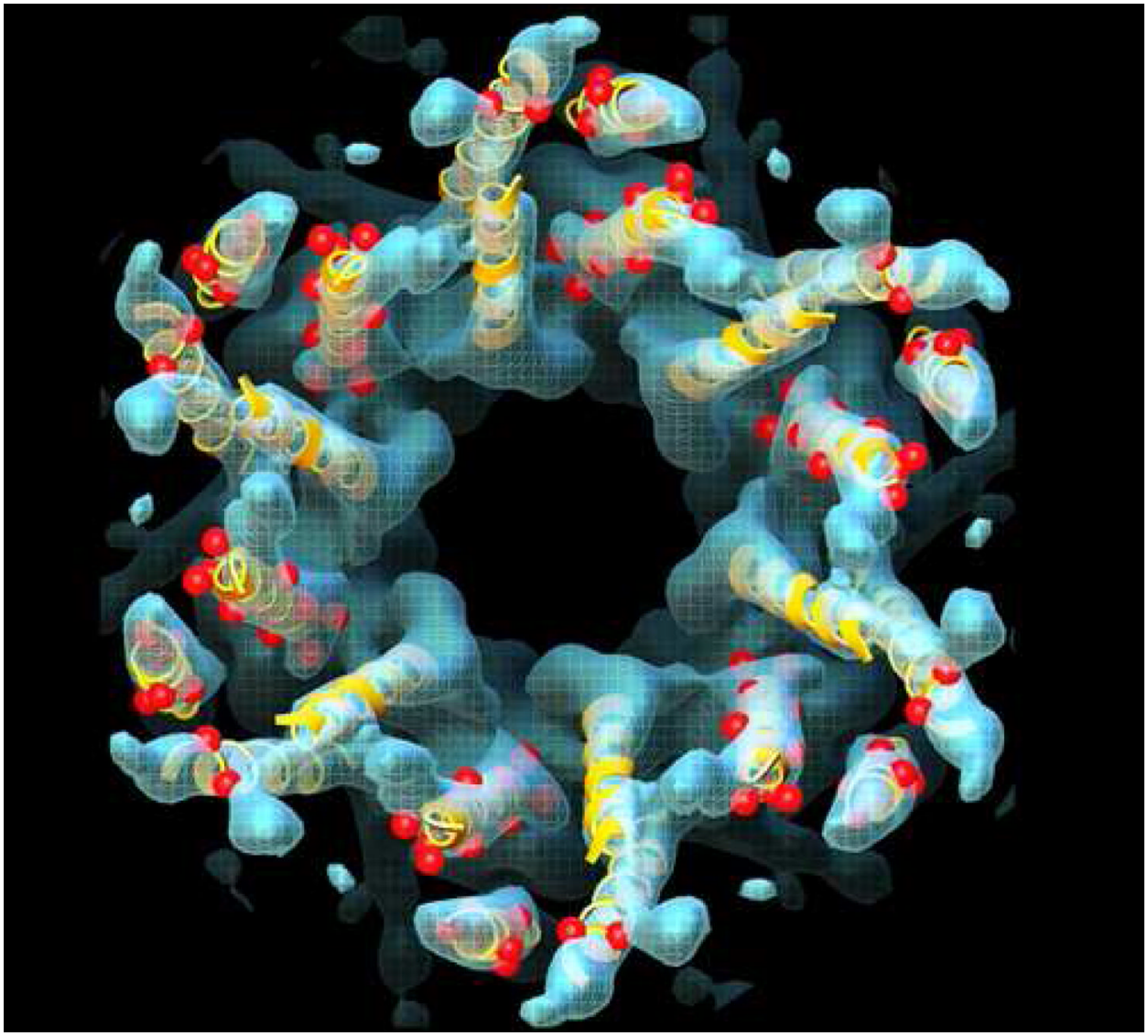

Figure 3.
A Cα model (yellow ribbons) for the membrane spanning α-helices of a connexon, derived by combining the information from a computational analysis of connexin sequences, the results of a number of biochemical studies, and the constraints provided by a 3D cryo-EM map (blue) [8]. While individually, none of these approaches provided high-resolution information, their sum yielded an atomic model that predicts how connexin mutations (red spheres) that result in diseases such as nonsyndromic deafness and Charcot-Marie-Tooth disease may interfere with formation of functional channels by disrupting helix-helix packing. Adapted from [8].

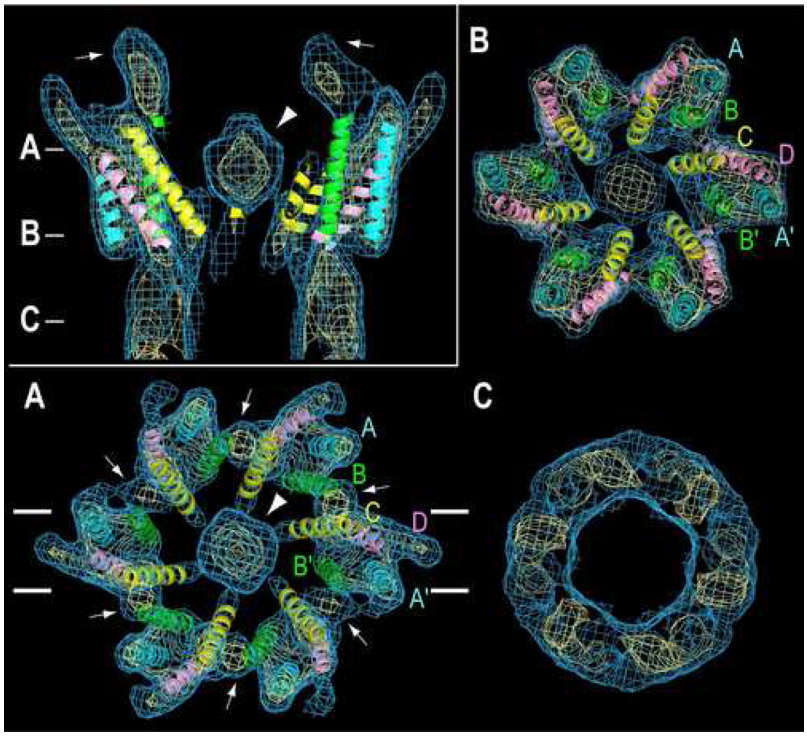

Figure 4.

CryoEM structure of two-dimensional crystals of reconstituted Cx26 connexons. The 3D map is contoured at 1σ (light blue) and 2.4 σ (yellow) above the mean density. The inset in the upper left shows a 20-Å-thick section perpendicular to the membrane plane through the density map of a connexon. This section corresponds to the region enclosed by the white lines shown in *A*. The arrowhead points to the large plug of density within the pore. The inner cytoplasmic protrusions (white arrows) extend from the cytoplasmic ends of helices B and C. (*A*–*C*). 30-Å-thick slabs through the density map corresponding to the position of the lines shown in the *Inset*. The four α-helices are labeled A (cyan, A′), B (green, B′), C (yellow), and D (pink) as in the original Cx43 structure (Figure 2) [7]. The arrowhead and white arrows represent the plug and the inner cytoplasmic protrusions, respectively, as in *Inset*. From [9], reproduced by permission.